

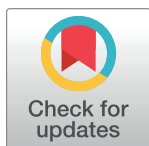
## RESEARCH ARTICLE

# The association of intra-therapeutic heterogeneity of somatostatin receptor expression with morphological treatment response in patients undergoing PRRT with [<sup>177</sup>Lu]-DOTATATE

Christoph Wetz<sup>1,2</sup>, Philipp Genseke<sup>1</sup>, Ivayla Apostolova<sup>3</sup>, Christian Furth<sup>2</sup>, Sammy Ghazzawi<sup>1</sup>, Julian M. M. Rogasch<sup>2</sup>, Imke Schatka<sup>2</sup>, Michael C. Kreissl<sup>1</sup>, Frank Hofheinz<sup>4</sup>, Oliver S. Grosser<sup>1</sup>, Holger Amthauer<sup>2\*</sup>

**1** Department of Radiology and Nuclear Medicine; University Hospital Magdeburg A.ö.R., Otto-von-Guericke University Magdeburg, Magdeburg, Germany, **2** Department of Nuclear Medicine, Charité-Universitätsmedizin Berlin, Berlin, Germany, **3** Department of Nuclear Medicine, University Medical Center Hamburg UKE, Hamburg, Germany, **4** Helmholtz-Zentrum Dresden-Rossendorf, Institute of Radiopharmaceutical Cancer Research, PET Center, Dresden, Germany

\* [holger.amthauer@charite.de](mailto:holger.amthauer@charite.de)



## OPEN ACCESS

**Citation:** Wetz C, Genseke P, Apostolova I, Furth C, Ghazzawi S, Rogasch JMM, et al. (2019) The association of intra-therapeutic heterogeneity of somatostatin receptor expression with morphological treatment response in patients undergoing PRRT with [<sup>177</sup>Lu]-DOTATATE. PLoS ONE 14(5): e0216781. <https://doi.org/10.1371/journal.pone.0216781>

**Editor:** Jason Chia-Hsun Hsieh, Chang Gung Memorial Hospital at Linkou, TAIWAN

**Received:** April 19, 2018

**Accepted:** April 29, 2019

**Published:** May 15, 2019

**Copyright:** © 2019 Wetz et al. This is an open access article distributed under the terms of the [Creative Commons Attribution License](https://creativecommons.org/licenses/by/4.0/), which permits unrestricted use, distribution, and reproduction in any medium, provided the original author and source are credited.

**Data Availability Statement:** All relevant data are within the paper.

**Funding:** The authors received no specific funding for this work.

**Competing interests:** The authors have declared that no competing interests exist.

## Abstract

### Aim

Purpose of this study was to evaluate the association of the spatial heterogeneity (asphericity, ASP) in intra-therapeutic SPECT/CT imaging of somatostatin receptor (SSR) positive metastatic gastroenteropancreatic neuroendocrine neoplasms (GEP-NEN) for morphological treatment response to peptide receptor radionuclide therapy (PRRT). Secondly, we correlated ASP derived from a pre-therapeutic OctreoScan (ASP<sub>[In]</sub>) and an intra-therapeutic [<sup>177</sup>Lu]-SPECT/CT (ASP<sub>[Lu]</sub>).

### Materials and methods

Data from first therapy cycle [<sup>177</sup>Lu-DOTA<sup>0</sup>-Tyr<sup>3</sup>]octreotate ([<sup>177</sup>Lu]-DOTATATE)-PRRT was retrospectively analyzed in 33 patients (m = 20; w = 13; median age, 72 [46–88] years). The evaluation of response to PRRT was performed according to RECIST 1.1 in responding lesions [RL (SD, PR, CR), n = 104] and non-responding lesions [NRL (PD), n = 27]. The association of SSR tumor heterogeneity with morphological response was evaluated by Kruskal-Wallis test and receiver operating characteristic curve (ROC). The optimal threshold for separation (RL vs. NRL) was calculated using the Youden-index. Relationship between pre- and intra-therapeutic ASP was determined with Spearman's rank correlation coefficient ( $\rho$ ) and Bland-Altman plots.

### Results

A total of 131 lesions (liver: n = 59, lymph nodes: n = 48, bone: n = 19, pancreas: n = 5) were analyzed. Lesions with higher ASP values showed a significantly poorer response to PRRT

(PD, median: 11.3, IQR: 8.5–15.5; SD, median: 3.4, IQR: 2.1–4.5; PR, median 1.7, IQR: 0.9–2.8; CR, median: 0.5, IQR: 0.0–1.3); Kruskal-Wallis,  $p < 0.001$ ). ROC analyses revealed a significant separation between RL and NRL for ASP after 4 months (AUC 0.85,  $p < 0.001$ ) and after 12 months (AUC 0.94,  $p < 0.001$ ). The optimal threshold for ASP was  $> 5.45\%$  (sensitivity 96% and specificity 82%). The correlation coefficient of pre- and intra-therapeutic ASP revealed  $\rho = 0.72$  ( $p < 0.01$ ). The mean absolute difference between ASP<sub>[In]</sub> and ASP<sub>[Lu]</sub> was -0.04 (95% Limits of Agreement, -6.1–6.0).

## Conclusion

Pre- and intra-therapeutic ASP shows a strong correlation and might be an useful tool for therapy monitoring.

## Introduction

Neuroendocrine neoplasms of the gastroenteropancreatic system (GEP-NEN) represents a rare and heterogeneous tumor entity. However, the incidence of GEP-NEN increased recently, mainly due to improved functional imaging and device-specific sensitivity [1]. Beyond commonly “cold” agents, such as somatostatin analogs, as a first-line antiproliferative drug, peptide receptor radionuclide therapy (PRRT) with [<sup>177</sup>Lu-DOTA<sup>0</sup>-Tyr<sup>3</sup>]octreotate ([<sup>177</sup>Lu]DOTA-TATE) has emerged as a highly effective treatment in metastatic well-differentiated GEP-NEN of low and intermediate grade G<sub>1</sub> and G<sub>2</sub>. [2, 3]. Several retrospective studies could also show the superiority of [<sup>177</sup>Lu]DOTA-TATE-PRRT in advanced inoperable GEP-NEN compared to other treatment modalities [4–6]. The recently published results of the first prospective randomized study in patients with progressive metastatic midgut NEN, NETTER-1, found a rate of 65.2% progression-free survival at month 20 after PRRT. In particular, the overall survival (OS) has not yet been reached in the study cohort [7]. In contrast, the current published ENETS guidelines recommend the use of PRRT in intestinal (midgut) NEN with distant and/or loco regional metastases as a second- to third-line therapy after progression under somatostatin-analogues (SSA) irrespective of the abovementioned NETTER-1 results. According to guidelines in pancreatic NEN with advanced locoregional disease PRRT should be even used as a third line therapy after failure of SSA, everolimus and/ or cytotoxic chemotherapy [8].

Meanwhile, application of PRRT can be only repeated to a limited extent, imposed by critical dose exposure in different organs at risk, e.g. in bone marrow ( $< 2\text{Gy}$ ) [9, 10] in 70% of patients after treatment with [<sup>177</sup>Lu]DOTA-TATE and in kidney ( $< 40\text{Gy}$ ) [11]. Histological diversities in metastatic SSR-expression are common findings, and may deliver objective prediction of therapy efficacy [12, 13]. However, not all patients benefit from PRRT. Therefore, better stratification criteria are highly desirable to identify patients with high probability for tumor response.

Until now, diagnosis and staging of NEN are merely based on analysis of tumor spread and morphology in imaging, irrespective of SSR expression and density.

Promising results have been published considering features from the non-invasive SSR-imaging that can be used separately or in combination to characterize more accurately biological behavior of NEN, thus leading to a better understanding of tumor/therapy response. The Krenning score, a well-established qualitative measure [3, 14], the metastases to liver ratio (M/L ratio), a first scanner-independent quantitative surrogate in [<sup>68</sup>Ga-DOTA<sup>0</sup>-Phe<sup>1</sup>-Tyr<sup>3</sup>]

octreotide (DOTATOC)-positron emission tomography (PET) combined with computed tomography (CT) [15], as well as the intratumoral SSR-heterogeneity in [<sup>68</sup>Ga]DOTATATE--PET/CT [16] represent the most common methodologies in prediction of response in PRRT. The assessment of asphericity (ASP), characterizing lesion's spatial SSR-heterogeneity e.g. by [<sup>111</sup>In-DTPA<sup>0</sup>]octreotide ([<sup>111</sup>In]octreotide, OctreoScan) scintigraphy [13], demonstrated an further promising parameter to predict response in PRRT planning [17]. Whereas, translation and verification of this novel image based methodology to intra-therapeutic workflow is missing.

The aim of the present study was to evaluate the predictive capability of tumoral SSR-receptor heterogeneity based on intra-therapeutic imaging with [<sup>177</sup>Lu]DOTATATE. Secondly, we correlated ASP derived from a pre-therapeutic OctreoScan (ASP<sub>[In]</sub>) and an intra-therapeutic [<sup>177</sup>Lu]DOTATATE-SPECT/CT imaging (ASP<sub>[Lu]</sub>).

## Materials and methods

### Patients

In this monocentric setting, data of all consecutive patients (n = 33; f, n = 13; m = 20; median age 72 ± 9.2 years, range, 46 to 88 years) treated by PRRT using [<sup>177</sup>Lu]DOTATATE were retrospectively included in the period from June 2011 to September 2015. The patients fulfilled the following inclusion criteria: (1) intra-therapeutic SPECT/CT (24 hours p.i.), (2) metastases could be clearly delineated on SPECT imaging (33/37 patients; 89%), (3) GEP-NEN was histologically proven, (4) patients underwent 2–4 cycles PRRT, (5) radiological follow up at least 12 months was available (33/41 patients; 80,5%). The assessment of tumor SSR-positivity was determined by [<sup>111</sup>In]octreotide SPECT/CT or [<sup>68</sup>Ga]DOTATOC-PET/CT prior to therapy. Further analysis was performed in a subset of twenty patients (f, n = 14; m = 6; median age 72 ± 7.4 years, range, 54 to 87 years) for a lesion-based correlation of ASP from pre-therapeutic [<sup>111</sup>In]octreotide SPECT/CT with intra-therapeutic SPECT/CT.

All patients provided written informed consent on the evaluation of their data, and approval from the institutional ethics committee of the Otto-von-Guericke-University (reference ID: RAD279; vote, 07/16) was obtained.

### <sup>177</sup>Lutetium—Peptide receptor radionuclide therapy (PRRT)

All patients underwent PRRT in concordance to the Rotterdam protocol and *The joint IAEA, EANM and SNMMI practical guidance* [18] as recently described [13]. In brief, patients obtained a <sup>177</sup>Lutetium-labelled (T<sub>1/2</sub> = 6.7d) synthetic somatostatin analogue, [DOTA<sup>0</sup>-Tyr<sup>3</sup>]octreotate. The patients were treated by two to four cycles (median, 3.3; IQR 3–4; range 2–4) of radionuclide therapy with a median administered activity of 200 mCi (7.4 GBq) [<sup>177</sup>Lu]DOTATATE per cycle. Follow up including both morphological contrast-enhanced CT (CE-CT) and functional imaging [<sup>111</sup>In]-OctreoScan, n = 12/33, 36%, or alternatively [<sup>68</sup>Ga]DOTATOC-PET/CT, n = 15/33, 64%, was obtained after the second and fourth cycle and 4 and 12 months, respectively. If interim staging indicated progressive disease, no further cycle of PRRT was administered [13].

### SPECT/CT imaging

Intra-therapeutic imaging was performed with a dual head SPECT/CT (Discovery NM/CT670, GE, Haifa, Israel) according to standard protocols. Planar imaging and SPECT with low-dose CT (X-ray tube current = 40 mAs) of thorax and abdomen for morphological correlation was carried out 24 hours p.i.. SPECT data were reconstructed by iterative algorithms

with CT-based correction for attenuation as previously described [13]. Imaging data was evaluated with a dedicated workstation (Xeleris-Workstation, GE Healthcare, Waukesha, USA) at standard clinical settings. Diagnostic CE-CT as well as contrast enhanced MRI of the liver was performed according to a standard protocol, published elsewhere [13, 19].

### Image analysis

Intra-therapeutic SPECT data sets were evaluated regarding SSR-heterogeneity in accumulation pattern as previously described [13]. In brief, SPECT data measured 24h p.i. at the first cycle [<sup>177</sup>Lu]-DOTATATE-PRRT was analyzed by a dedicated software (ROVER version 2.1.20, ABX, Radeberg, Germany). The functional tumor volume, a measure of the SSR uptake of tumor tissue, was delineated by a semi-automatic algorithm based on adaptive threshold taking the local background into account [20, 21]. For the resulting volumes of interest (VOI) the ASP was computed using the following equation:

$$ASP = \sqrt[3]{H} - 1 \text{ with } H = \frac{1}{36\pi} \frac{S^3}{V^2}$$

where S and V are the mean surface and volume of the lesions' functional active part, respectively. The ASP described the deviation of an activity accumulation from spherical geometry. A small ASP (Range 1–5%) represents a more spherical accumulation while increasing ASP represents considerably deviating pattern (e.g. elliptical). A more detailed description has been given in recent studies [13, 22].

For lesion based analysis the heterogeneity of lymph-node-, bone-, liver- as well as pancreatic- metastases were assessed to ensure a systemic and not organ-based approach. According to the response evaluation criteria in solid tumors (RECIST 1.1) only two lesions per organ and not more than five per patient were included. In the case of more than two metastases per organ ASP was derived from two individual lesions with the most representative SSR-uptakes on visual assessment.

The association between ASP and results from RECIST-evaluation was evaluated for three different time points (pre PRRT: mean = 4 weeks, range: 1–9 weeks), 4 months post PRRT, and 12 months post PRRT). In generally, morphological assessment was performed by CE-CT. Alternatively, CE-MRI was used for morphological evaluation (contrast-enhanced, CE-MRI; n = 23/33 70%) if available. Analysis of the CE-CT (CE-MRI) data was performed using dedicated radiologic workstation INFINITT (INFINITT Healthcare Co., Ltd., Seoul, South Korea). In order to permit comparison with CE-CT, generally the short axis of lymph-nodes and long diameters in the transverse plane for liver, pancreatic and bone metastases were drawn. Lesions with a short axis of <15 mm (lymph nodes) and <10 mm (pancreas, liver lesions, bone lesions) were not included into analysis to avoid partial volume effects. The morphological changes in diameter were classified according to the RECIST 1.1 guidelines. Definition of VOIs and calculation of the diameter were performed in consensus by two physicians. The different classes were further cumulated in responding lesions (RL [SD, PR, CR], n = 104) and non-responding lesions (NRL [PD], n = 27). The rationale for this definition was published elsewhere [23].

### Statistical analysis

Data analyses were performed using SPSS 22 (IBM Corp., Armonk, NY, USA). Descriptive values were expressed as median, interquartile range (IQR, 25th percentile–75th percentile), and range (minimum–maximum) and depicted as boxplots. According to histograms and quantile-quantile plots, the distribution of data-sets was assumed non-parametric. The ASP within

the context of intra-therapeutic dosimetry was analyzed using the Kruskal-Wallis test and receiver operating characteristic curve (ROC). The optimal threshold for separation of RL and NRL was calculated using the Youden’s index [24].

The cutoff values were assessed separately for prediction response at 4 and 12 months post PRRT. ASP values was binarized using ROC cutoffs and the associated sensitivity and specificity were determined. Statistical significance was assumed at a *P* value < 0.05 and high significance at *P* value < 0.001. A subanalysis was performed in patients who underwent a pretherapeutic [<sup>111</sup>In]octreotide SPECT/CT. The correlation of ASP<sub>[In]</sub> and ASP<sub>[Lu]</sub> was compared by Spearman’s rank correlation coefficient rho ( $\rho$ ) and the limits of agreement were determined in a Bland-Altman diagram. Concordance was assumed at a deviation of  $\leq 5\%$ .

## Results

Of the 33 patients, 10/33 (30.3%) patients had a GEP-NEN including the primary tumor of the foregut (stomach, pancreas and duodenum); in 13/33 (39.4%) patients, the primary occurred in the midgut (jejunum, ileum, and proximal colon); in 5/33 (15.2%) patients, the tumor origin was localized in the hindgut (the remaining two thirds of colon and rectum). 5/33 (15.2%) patients suffered from cancer of unknown primary (CUP). All NENs were well differentiated, low (G<sub>1</sub>) to intermediate (G<sub>2</sub>) grade. Antigen Ki-67, the proliferation index, ranged from 1–17% (median 4%). Chromogranin A (CgA) levels ranged between 94–12600 µg/l (median 632). All patients showed inoperable, metastasized NEN and had undergone different treatment modalities such as surgical intervention (n = 29/33, 87.9%), somatostatin analogue therapy (n = 31/33, 93.9%) or chemotherapy (n = 6/33, 18.2%). Routinely acquired patient data and characteristics are illustrated in Table 1.

A total of 131 lesions (liver: n = 59, lymph nodes: n = 48, bone: n = 19, pancreas: n = 5) were analyzed. Of the 131 lesions, 104 lesions had been assigned to the RLs and 27 to the NRLs

**Table 1. Patient data and therapy characteristics.**

Characteristic		Value
<b>Primary</b>		<b>33 (100%)</b>
	<b>GEP-NEN Total (n)</b>	
	foregut	10 (30.3%)
	midgut	13 (39.4%)
	hindgut	5 (15.15%)
	<b>CUP-NEN (n)</b>	<b>5 (15.15%)</b>
<b>Metastatic spread</b>	<b>NEN-(Mx) (n)</b>	<b>131 (100%)</b>
	hepatic	59 (45.0%)
	lymphnode	48 (36.6%)
	bone	19 (14.6%)
	pancreatic	5 (3.8%)
<b>Ki-67 (%)*</b>		6* (range, 1–17)
<b>Chromogranin A* (µg/l)</b>		632* (range, 94–12600)
<b>PRRT</b>	Number of cycles	3.3* (IQR, 3–4)
	Administered dose	200 mCi (7,4 GBq)

Detailed therapy and patient characteristics in systematic overview: *GEP-NEN*, gastro-enteropancreatic neuroendocrine neoplasm; *CUP-NEN*, neuroendocrine neoplasm of unknown primary

\* = median and range/ *IQR*, interquartile range; *PRRT*, peptide receptor radionuclide therapy; *GBq*, gigabequerel, *mCi*, millicurie.

<https://doi.org/10.1371/journal.pone.0216781.t001>

according to morphologic assessment [23]. There was no significant difference in the functional tumor volume (FTV) between both response groups prior treatment with [ $^{177}\text{Lu}$ ]DOTATATE-PRRT ( $p > 0.05$ ).

### Lesion response

Assessment of the pre-therapeutic lesion diameters revealed 19.2 mm (IQR, 13.7–33.3 mm; range, 10.0–100.0 mm) for RL and 19.6 mm (IQR, 14.2–35.0 mm; range, 12.0–104.6 mm) for NRL. After 4-month follow up analyses of the RLs showed a significantly decreased median lesion size in RL of 16.9 mm (IQR, 13.0–29.5; range, 0.0–75.0;  $p < 0.001$ ). Assessment of the NRLs demonstrated a significant increase in diameter to 23.2 mm (IQR, 16.1–40.0; range, 10.0–124.6;  $p < 0.001$ ). Kruskal-Wallis test depicted a highly significant difference in the diameter of RLs and NRLs after two cycles, i.e. 4-months, of [ $^{177}\text{Lu}$ ]DOTATATE-PRRT (16.9 mm; IQR, 13.0–29.5 vs. 23.2 mm; IQR, 16.1–40.0;  $p < 0.001$ ).

After 12 months follow-up, the median lesion size in RLs showed a reduction in diameter to 13.9 mm (IQR, 10.2–24.0; range, 0.0–63.0). The median lesion size in NRLs increased to 29.0 mm (IQR, 19.0–49.0; range, 15.0–136.4) after treatment. A highly significant difference was detected in the diameter of RLs and NRLs compared at initial measurement and after treatment (13.9 mm; IQR, 10.2–24.0 vs. 29.0 mm; IQR, 19.0–49.0;  $p < 0.001$ ).

[Fig 1](#) presents a typical example of an RL, and a representative case of an NRL.

### Potential predictive relevance of ASP

Lesions with high  $\text{ASP}_{[\text{Lu}]}$  showed a significantly poorer response to PRRT: PD, 11.3 (IQR: 8.5–15.5; range, 2.4–21.3); SD, 3.4 (IQR: 2.1–4.5; range, 0.2–18.0). PR, 1.7 (IQR: 0.9–2.8; range, 0.0–5.5). CR, 0.5 (IQR: 0.0–1.3; range, 0.0–2.8; Kruskal-Wallis,  $p < 0.001$ ; [Fig 2A and 2C](#)).

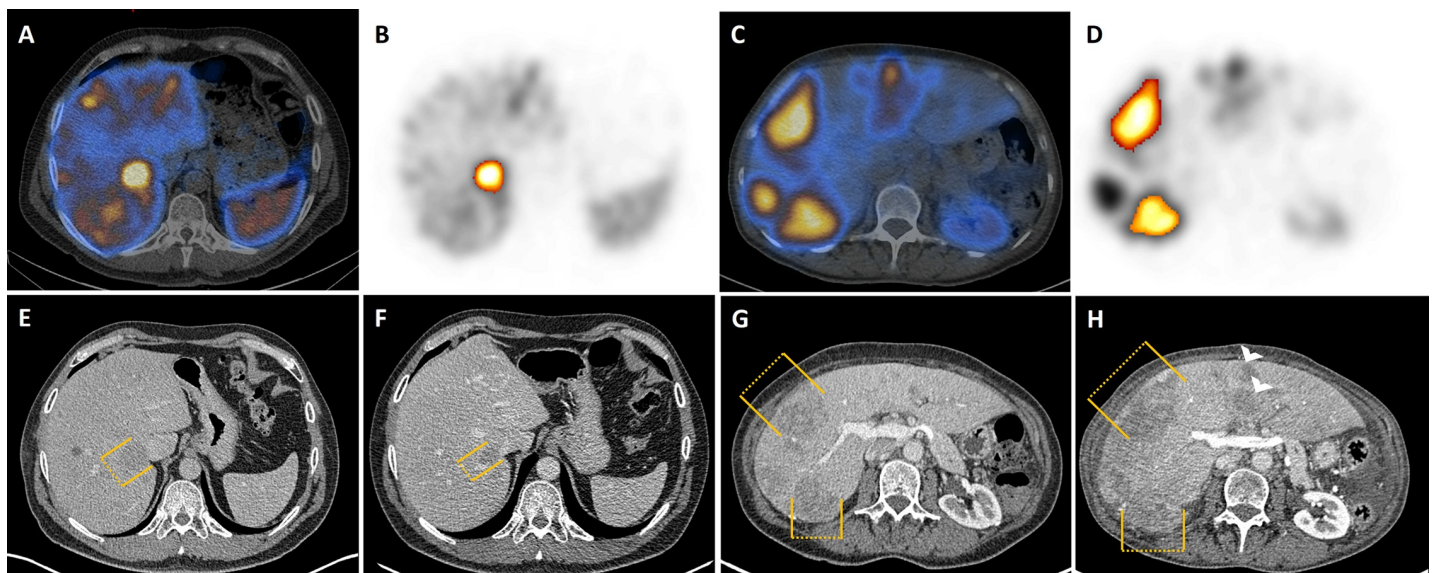


**Fig 1. Representative responding lesion (RL) and non-responding lesion (NRL).** Baseline SPECT/CT during dosimetry (24h p.i.). Representative example of one responding lesion in liver segment VI (A) of a 48-year-old man suffering from metastatic duodenal NEN. The lesion can be detected on SPECT (B) and is illustrated by orange bars on CT at baseline (E) and after 12 months follow-up (F). The lesion decreased from 3.9 cm with a functional SPECT-volume of 19.7 ml to 2.3 cm after 4 cycles' [ $^{177}\text{Lu}$ ]DOTATATE-PRRT and 12 months follow-up, respectively. Images (C,D,G,H) showing a typical example of non-responding lesions. A 59-year-old woman suffering from pancreatic (P)-NEN with predominant liver metastases. Hepatic metastases can be detected on CT (G) as well as on SPECT (D) and image fusion, SPECT/CT (C). The lesions' measurements are displayed by orange bars. Two exemplary lesions in liver segment VII and VIII (G) are shown with a maximum diameter of 3.5 cm (functional tumor volume [FTV] 26.4 ml) and 4.6 cm (FTV 34.0 ml) prior to treatment. After two cycles of [ $^{177}\text{Lu}$ ]DOTATATE-PRRT, tumor diameters increased to 4.2 cm (segment VII) and 7.0 cm (segment VIII). As an additional finding, new metastases are highlighted with white arrow heads (H).

<https://doi.org/10.1371/journal.pone.0216781.g001>

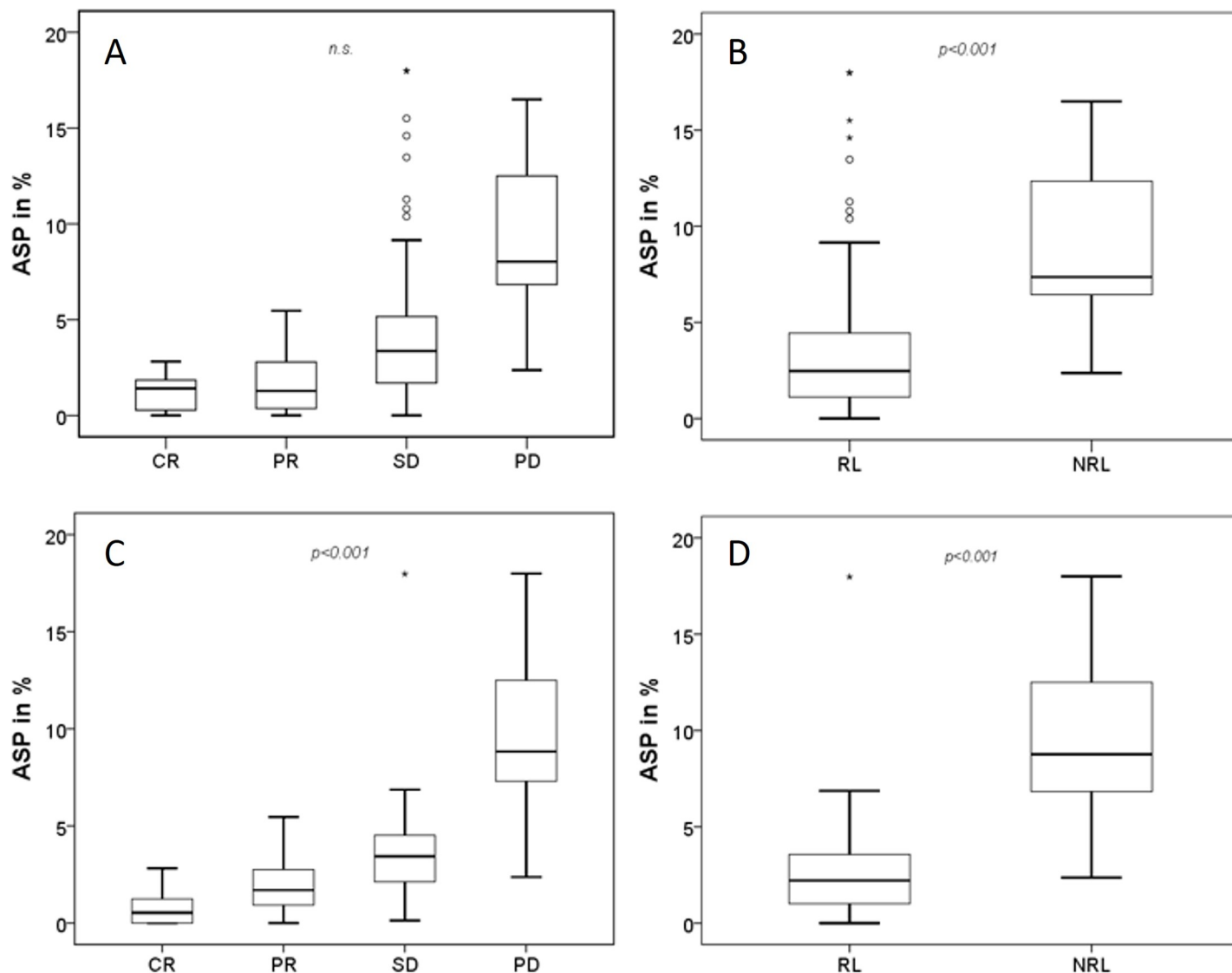


**Fig 2. Box plot analysis of ASP.** ASP clustered by RECIST criteria after (A) 4 and (C) 12-months follow-up. B and D shows ASP for responding (RL) and non-responding lesions (NRL) for the corresponding follow-up examinations at 4 and 12 months, respectively.

<https://doi.org/10.1371/journal.pone.0216781.g002>

Mann-Whitney U test analysis revealed a significantly lower ASP<sub>[Lu]</sub> in RLs (2.9%; IQR, 0.9–3.9; range, 0.0–18.0) compared to NRLs (11.3%; IQR, 8.5–15.5; range, 2.4–21.3;  $p < 0.001$ ; Fig 2B and 2D)

Receiver Operating Characteristics (ROC) analysis revealed the highest area under the curve (AUC) for ASP to separate between RLs and NRLs after 4 months (AUC 0.85,  $p < 0.001$ ). The optimal cutoff value from ROC analysis was 6.39% (sensitivity and specificity, 77.0 and 88.0%; Fig 3). According to ROC-analysis, ASP after 12 months showed a highly significant AUC of 0.94 ( $p < 0.001$ ) to differentiate between the two response groups. The optimal cutoff for ASP was  $> 5.45\%$  (sensitivity and specificity, 96.0% and 82.0%, respectively; Fig 3).

### Correlation of ASP<sub>[In]</sub> and ASP<sub>[Lu]</sub>

From the overall cohort of 33 patients, 20 patients, containing a pre-therapeutic [<sup>111</sup>In]octreotide SPECT/CT (77 lesions; liver:  $n = 60$ , lymph nodes:  $n = 11$ , bone:  $n = 4$ , pancreas:  $n = 2$ )

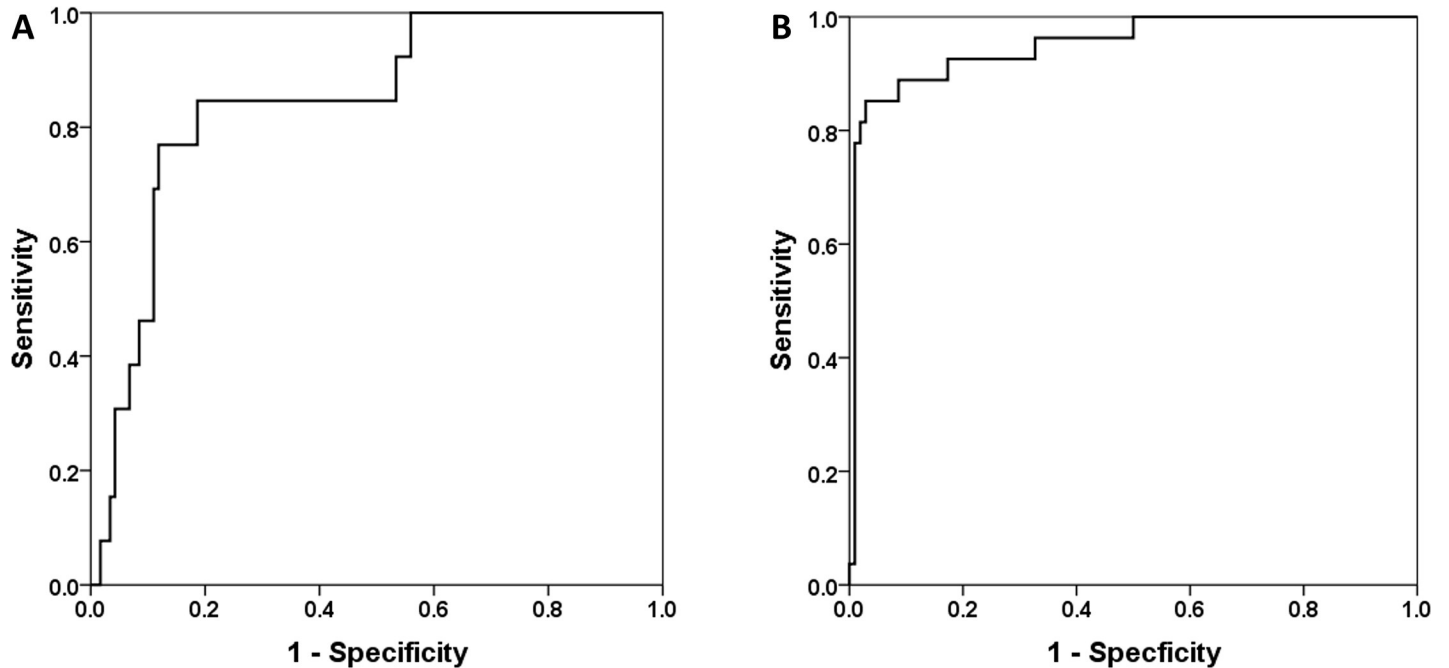


**Fig 3. ROC curve comparison—4 and 12 months follow-up.** ROC for the association of ASP with morphological treatment response (measures 4 months post first PRRT revealed an AUC = 0.85,  $p < 0.001$ ; A). The optimal cutoff for ASP in prediction of NRL was  $>6.39\%$  (sensitivity and specificity, 77.0% and 88.0%). After 12 months (B), ASP showed an AUC of 0.94,  $p < 0.001$ . The optimal cutoff for ASP was  $>5.45\%$  (sensitivity and specificity, 96% and 82%).

<https://doi.org/10.1371/journal.pone.0216781.g003>

were analyzed in a subgroup. The optimal threshold for the pre-PRRT estimated  $ASP_{[In]}$  was  $<5.12\%$  (sensitivity 90% and specificity 93%) and for the intra-therapeutically estimated  $ASP_{[Lu]} <5.02\%$  (sensitivity 92% and specificity 89%). The correlation coefficient was  $\rho = 0.72$  ( $p < 0.01$ , Fig 4). The mean absolute difference between  $ASP_{[In]}$  and  $ASP_{[Lu]}$  was  $-0.04\%$  (95% Limits of Agreement,  $-6.1-6.0$ ). 10/77 lesions (7/60 liver, 1/10 lymph nodes, 2/6 others) were discordant (absolut difference  $>5\%$ ).

## Discussion

In this retrospective study, we investigated the spatial heterogeneity (ASP) in SSR-positive/functional metastatic GEP-NEN, using intra-therapeutic SPECT/CT data derived from the first cycle PRRT. Using this methodology we showed a strong association of ASP with morphological treatment response in patients undergoing PRRT with  $[^{177}Lu]$ -DOTATATE. Even in diagnostic and in therapeutic imaging using  $[^{111}In]$ -OctreoScan or  $[^{177}Lu]$ -PRRT we demonstrated a strong correlation, resulting in high sensitivity and specificity.

A number of studies have already dealt with different texture analyses aimed at differentiation between benign and malignant lesions [25]. The tumor heterogeneity in lung carcinoma was evaluated by CT texture analysis. Considering a quite good contrast in lung tissue the quantification within lung tumors can be easily assessed. However, this is not the case within liver or other organ lesions. Here CT delineation would be more challenging until semi-automatic segmentation of tumor delineation is limited due to worse tissue contrast in CT images. Lesions have to be evaluated in a manually, volumetric analysis—slice by slice. MRI delivers a better soft tissue contrast and the potential for accurate segmentation of metastases in the liver and other organs, respectively. Besides, several other studies worked with texture oriented analysis of morphologic data from CT or MRI in various entities (e.g. lung carcinoma [26] or



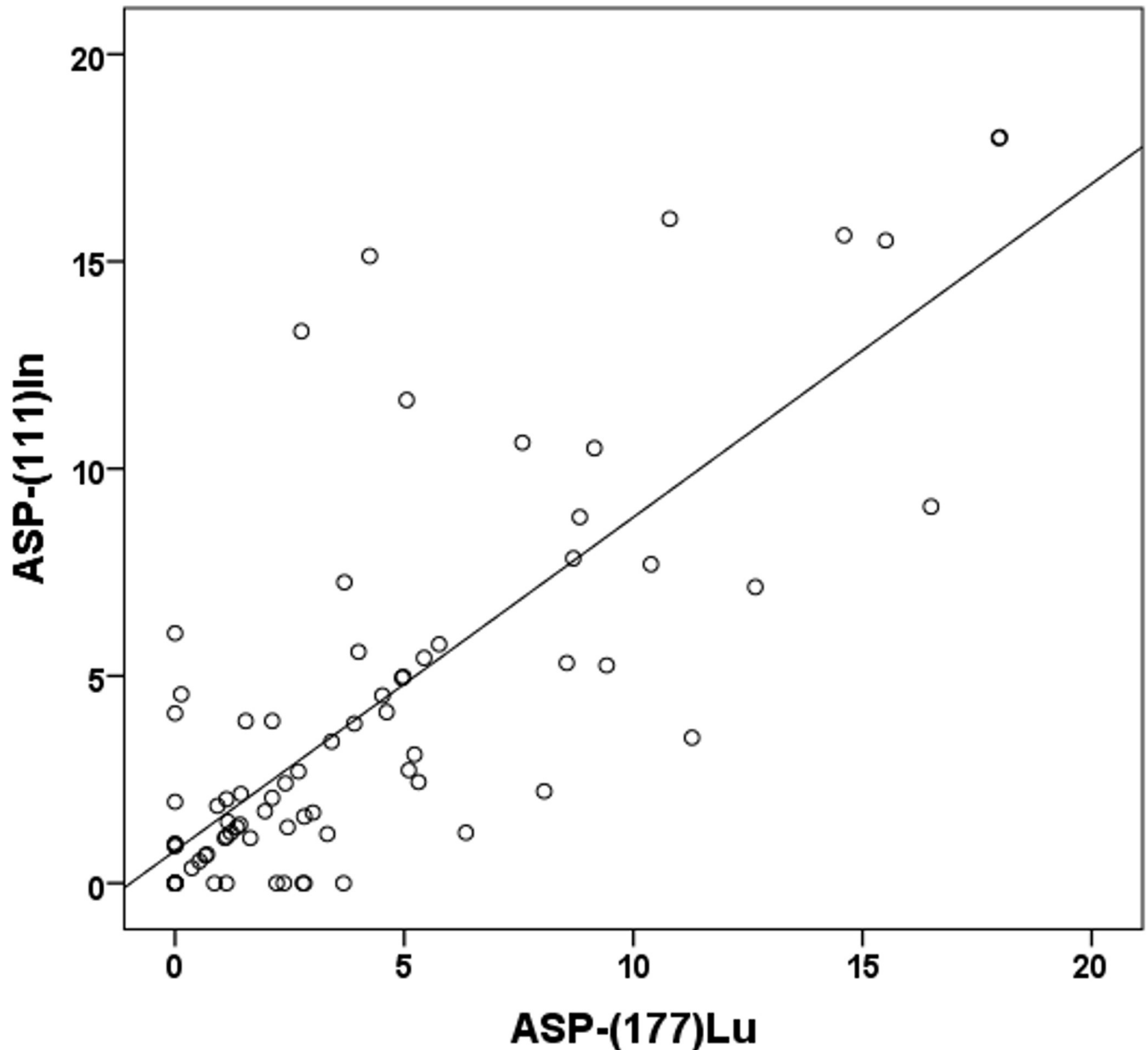


**Fig 4. Spearman's rank correlation  $ASP_{[In]}$  and  $ASP_{[Lu]}$ .** Scatterplot showing the correlation of ASP estimated from pre-therapeutic [ $^{111}In$ ]-octreotide SPECT/CT [ $ASP-(111)In$ ] and intra-therapeutic ASP [ $ASP-(177)Lu$ ] ( $\rho = 0.72$ ,  $p < 0.01$ ).

<https://doi.org/10.1371/journal.pone.0216781.g004>

colorectal cancer [27]), our analysis was based on SSR expression estimated by functional imaging. The predictive and prognostic importance of metabolic spatial heterogeneity of tumor lesions was also demonstrated for different cancer types e.g. using 18F-fluorodeoxyglucose (FDG)-PET/CT with partly promising results [22, 28]. Corresponding observations have also been published by Werner et al. who reported on the tumor entropy as a surrogate parameter assessed by [ $^{68}Ga$ ]DOTATATE- or [ $^{68}Ga$ ]DOTATOC-PET/CT in patients with late-stage GEP-NEN prior PRRT [16].

Heterogeneity was the favored parameter in distinction between responder and non-responder. In particular, heterogeneity parameters (such as homogeneity, correlation, size

variation and short zone emphasis and “entropy” with the highest AUC of 0.70) outperformed conventional parameters like standardized uptake value (SUV) and total receptor expression. In line with these findings, heterogeneity analysis of thyroid cancer showed only significant results in a patient-based setting. Despite our results, in a lesion based analysis only the parameter “entropy” demonstrated with an AUC of 0.73 and a definitely lower sensitivity of 67% and a specificity of 75% response prediction [29]. For adequate therapy-monitoring lesion-based control is always preferable compared to patient-based follow-up. In NEN the mitotic count (MC) and Ki-67 are the most common and reliable biomarkers for cell-proliferation and thus, indicators for biological phenotypes [30, 31]. Although MC was used as the biomarker for GEP-NEN during the last decades, finally Khan et al. [32] showed the disparity of MC and Ki-67 and favored Ki-67 as a prognostic marker in grading. Actual Ki-67 plays the major role in dividing GEP-NEN into different grades of disease ( $G_{1-3}$  NEN/  $G_3$ -NEC) which directly affects therapy management [33]. Unfortunately, the Ki-67, as a prognostic marker, delivers some pitfalls, physicians have to be aware of. Assessment of Ki-67 depends on expertise of the reporting pathologist [34] and core biopsies represent only a small tumor sample, which impedes accurate heterogeneity assessment, especially of intermediate  $G_2$ -lesion [35]. Lastly, Ki-67 index is known to fluctuate in some patients, not only with the choice of therapy but also during the time of treatment [36, 37]. Considering these findings, non-invasive and reliable whole-body assessment of inter-lesional heterogeneity may reflect the whole tumor burden in a more representative way—taking the divergent tumor areas into account. Even the well-established urine and serum-based parameters for treatment monitoring and follow-up, such as 5-hydroxyindole acetic acid (5-HIAA) [37] and Chromogranin A (CgA) [38], failed as prognostic biomarker. Since 18–33% of all patients with metastatic GEP-NEN show PD after PRRT, ASP might deliver a reliable surrogate parameter in selecting potential non-responder [39, 40]. Especially, those patients can benefit from an early therapy-switch. Applying the ASP in pre-therapeutic octreotide-scintigraphy, we could recently demonstrate that low ASP predicts response to PRRT [13]. However, when dealing with elaborative predictive parameters, it is advantageous to use comparable DOTA-conjugates, such as intra-therapeutic [ $^{177}\text{Lu}$ -DOTA $^0$ , Tyr $^3$ ]octreotate, with equal SSR-affinity to ensure robustness of the test and to minimize varieties.

Nevertheless, subgroup analysis presented a high correlation of  $\text{ASP}_{[\text{In}]}$  and  $\text{ASP}_{[\text{Lu}]}$  and thus, validated the method. The marginal better area under the curve for ASP, obtained in pre-therapeutic SPECT/CT imaging, might have been affected by a smaller study population bias.

More recently, functional imaging of NEN with  $^{68}\text{Ga}$ -labelled DOTA analogues (e.g., TATE/ TOC/ NOC) is the preferred SSR-imaging in follow-up examinations, due to better sensitivity, spatial resolution and less radiation [41]. Although there is still limited data available regarding PET-based follow-up, the ENETS consensus guidelines recommend MRI/ CT every 3–12 months and a receptor imaging in  $G_{1-2}$  P-NEN each 12–24 months after treatment. If there is progression suspected, even anytime earlier [42]. Moreover, the post-therapeutic scan is performed during therapeutic procedure (e.g. for dosimetry) immediately after treatment (24 h p.i.). Providing an early surrogate for tumor response from analyzing. Our results suggest that ASP may deliver a strong approach in intra-therapeutic risk monitoring, indicating that follow-up intervals, e.g. CT every 3–12 months, [ $^{68}\text{Ga}$ ]DOTANOC-PET/CT every 12–24 months, can be even prolonged. An encouraging aspect is the synergistic character of the ASP evaluation. ASP analysis uses functional data from standard diagnostics in patients with GEP-NEN or from dosimetry (in treatment validation) providing benefits without an additional test.

Different limitations may arise: Contrary to other qualitative visual scores, the ASP may deliver a semi-automatic parameter, which ensures reproducibility and robustness in

prediction response. Nevertheless, the ASP is not a scanner independent surrogate parameter. It can be hypothesized that ASP is in small lesion affected by partial volume effect. Mainly due to remarkable progress in functional imaging and resolution, lesions smaller than 2.5ml [22], which used to appear with symmetrical sphere shape, can be depicted these days in less than a few millimeters in size. Thus, modern SPECT-devices, such as cadmium-zinc-telluride (CZT) detectors, exhibit a higher spatial resolution [43]. This might avoid adulteration of the ASP in smaller lesions. The limitations of our study are the small sample size, no comparison group and retrospective design. Nevertheless, considering GEP-NEN are commonly rare tumor entity [1], we were able to provide valuable findings and demonstrate significant effects that show some support for our hypotheses. However, further validation of ASP as a potential predictive marker is still required.

## Conclusion

Pre- and intra-therapeutic ASP shows a strong correlation with morphological treatment response and might represent a potential predictive marker for PRRT. Further assessment of its predictive value is worthwhile and might improve therapeutic decision making in NEN.

## Acknowledgments

We thank the staff and participants at the Department of Radiology and Nuclear Medicine, University Hospital Magdeburg and the Department of Nuclear Medicine, Charité-Universitätsmedizin Berlin for kind support.

## Author Contributions

**Conceptualization:** Christoph Wetz, Ivayla Apostolova, Oliver S. Grosser, Holger Amthauer.

**Data curation:** Philipp Genseke, Sammy Ghazzawi, Julian M. M. Rogasch, Frank Hofheinz.

**Methodology:** Christoph Wetz, Philipp Genseke, Ivayla Apostolova, Julian M. M. Rogasch, Frank Hofheinz, Oliver S. Grosser, Holger Amthauer.

**Project administration:** Christoph Wetz.

**Supervision:** Christian Furth, Imke Schatka, Michael C. Kreissl, Holger Amthauer.

**Writing – original draft:** Christoph Wetz.

**Writing – review & editing:** Oliver S. Grosser, Holger Amthauer.

## References

1. Hallet J, Law CHL, Cukier M, Saskin R, Liu N, Singh S. Exploring the rising incidence of neuroendocrine tumors: A population-based analysis of epidemiology, metastatic presentation, and outcomes. *Cancer*. 2015; 121(4):589–97. <https://doi.org/10.1002/cncr.29099> PMID: 25312765
2. Van Essen M, Krenning EP, De Jong M, Valkema R, Kwekkeboom DJ. Peptide receptor radionuclide therapy with radiolabelled somatostatin analogues in patients with somatostatin receptor positive tumours. *Acta Oncologica*. 2007; 46(6):723–34. <https://doi.org/10.1080/02841860701441848> PMID: 17653893
3. Kwekkeboom DJ, Teunissen JJ, Bakker WH, Kooij PP, de Herder WW, Feelders RA, et al. Radiolabeled somatostatin analog [177Lu-DOTA0, Tyr3] octreotate in patients with endocrine gastroenteropancreatic tumors. *Journal of Clinical Oncology*. 2005; 23(12):2754–62. <https://doi.org/10.1200/JCO.2005.08.066> PMID: 15837990
4. Ezziddin S, Khalaf F, Vanezi M, Haslerud T, Mayer K, Al Zreiqat A, et al. Outcome of peptide receptor radionuclide therapy with 177Lu-octreotate in advanced grade 1/2 pancreatic neuroendocrine tumours. *European journal of nuclear medicine and molecular imaging*. 2014; 41(5):925–33. <https://doi.org/10.1007/s00259-013-2677-3> PMID: 24504504

5. Bodei L, Cremonesi M, Grana CM, Fazio N, Iodice S, Baio SM, et al. Peptide receptor radionuclide therapy with <sup>177</sup>Lu-DOTATATE: the IEO phase I-II study. *European journal of nuclear medicine and molecular imaging*. 2011; 38(12):2125–35. <https://doi.org/10.1007/s00259-011-1902-1> PMID: 21892623
6. Khan S, Krenning EP, van Essen M, Kam BL, Teunissen JJ, Kwekkeboom DJ. Quality of life in 265 patients with gastroenteropancreatic or bronchial neuroendocrine tumors treated with [<sup>177</sup>Lu-DOTA<sub>0</sub>, Tyr<sub>3</sub>] octreotate. *Journal of nuclear medicine*. 2011; 52(9):1361–8. <https://doi.org/10.2967/jnumed.111.087932> PMID: 21795361
7. Strosberg J, El-Haddad G, Wolin E, Hendifar A, Yao J, Chasen B, et al. Phase 3 Trial of <sup>177</sup>Lu-Dotatate for Midgut Neuroendocrine Tumors. *New England Journal of Medicine*. 2017; 376(2):125–35. <https://doi.org/10.1056/NEJMoa1607427> PMID: 28076709
8. Pavel M, O'Toole D, Costa F, Capdevila J, Gross D, Kianmanesh R, et al. ENETS Consensus Guidelines Update for the Management of Distant Metastatic Disease of Intestinal, Pancreatic, Bronchial Neuroendocrine Neoplasms (NEN) and NEN of Unknown Primary Site. *Neuroendocrinology*. 2016; 103(2):172–85. <https://doi.org/10.1159/000443167> PMID: 26731013
9. de Jong M, Kwekkeboom D, Valkema R, Krenning EP. Radiolabelled peptides for tumour therapy: current status and future directions. *European journal of nuclear medicine and molecular imaging*. 2003; 30(3):463–9. <https://doi.org/10.1007/s00259-002-1107-8> PMID: 12569416
10. Cremonesi M, Ferrari M, Zoboli S, Chinol M, Stabin MG, Orsi F, et al. Biokinetics and dosimetry in patients administered with <sup>111</sup>In-DOTA-Tyr 3-octreotide: implications for internal radiotherapy with <sup>90</sup>Y-DOTATOC. *European Journal of Nuclear Medicine and Molecular Imaging*. 1999; 26(8):877–86.
11. Bodei L, Cremonesi M, Ferrari M, Pacifici M, Grana CM, Bartolomei M, et al. Long-term evaluation of renal toxicity after peptide receptor radionuclide therapy with <sup>90</sup>Y-DOTATOC and <sup>177</sup>Lu-DOTATATE: the role of associated risk factors. *European journal of nuclear medicine and molecular imaging*. 2008; 35(10):1847–56. <https://doi.org/10.1007/s00259-008-0778-1> PMID: 18427807
12. Davnall F, Yip CS, Ljungqvist G, Selmi M, Ng F, Sanghera B, et al. Assessment of tumor heterogeneity: an emerging imaging tool for clinical practice? *Insights into imaging*. 2012; 3(6):573–89. <https://doi.org/10.1007/s13244-012-0196-6> PMID: 23093486
13. Wetz C, Apostolova I, Steffen I, Hofheinz F, Furth C, Kupitz D, et al. Predictive Value of Asphericity in Pretherapeutic [<sup>111</sup>In] DTPA-Octreotide SPECT/CT for Response to Peptide Receptor Radionuclide Therapy with [<sup>177</sup>Lu] DOTATATE. *Molecular Imaging and Biology*. 2016:1–9.
14. Hofman MS, Lau WE, Hicks RJ. Somatostatin receptor imaging with <sup>68</sup>Ga DOTATATE PET/CT: clinical utility, normal patterns, pearls, and pitfalls in interpretation. *Radiographics*. 2015; 35(2):500–16. <https://doi.org/10.1148/rg.352140164> PMID: 25763733
15. Kratochwil C, Stefanova M, Mavriopoulou E, Holland-Letz T, Dimitrakopoulou-Strauss A, Afshar-Oromieh A, et al. SUV of [<sup>68</sup>Ga] DOTATOC-PET/CT predicts response probability of PRRT in neuroendocrine tumors. *Molecular Imaging and Biology*. 2015; 17(3):313–8. <https://doi.org/10.1007/s11307-014-0795-3> PMID: 25319765
16. Werner RA, Lapa C, Ilhan H, Higuchi T, Buck AK, Lehner S, et al. Survival prediction in patients undergoing radionuclide therapy based on intratumoral somatostatin-receptor heterogeneity. *Oncotarget*. 2017; 8(4):7039–49. Epub 2016/10/06. <https://doi.org/10.18632/oncotarget.12402> PMID: 27705948; PubMed Central PMCID: PMC5351689.
17. Bakker W, Albert R, Bruns C, Breeman W, Hofland L, Marbach P, et al. [<sup>111</sup>In-DTPA-D-Phe<sup>1</sup>]-octreotide, a potential radiopharmaceutical for imaging of somatostatin receptor-positive tumors: synthesis, radiolabeling and in vitro validation. *Life sciences*. 1991; 49(22):1583–91. PMID: 1658515
18. Zaknun JJ, Bodei L, Mueller-Brand J, Pavel M, Baum R, Horsch D, et al. The joint IAEA, EANM, and SNMMI practical guidance on peptide receptor radionuclide therapy (PRRT) in neuroendocrine tumours. *European journal of nuclear medicine and molecular imaging*. 2013; 40(5):800–16. <https://doi.org/10.1007/s00259-012-2330-6> PMID: 23389427
19. Pech M, Mohnike K, Wieners G, Bialek E, Dudeck O, Seidensticker M, et al. Radiotherapy of liver metastases. *Strahlentherapie und Onkologie*. 2008; 184(5):256–61. <https://doi.org/10.1007/s00066-008-1849-8> PMID: 18427756
20. Hofheinz F, Pöttsch C, Oehme L, Beuthien-Baumann B, Steinbach J, Kotzerke J, et al. Automatic volume delineation in oncological PET. *Nuklearmedizin*. 2012; 51(01):9–16.
21. Hofheinz F, Langner J, Petr J, Beuthien-Baumann B, Steinbach J, Kotzerke J, et al. An automatic method for accurate volume delineation of heterogeneous tumors in PET. *Medical physics*. 2013; 40(8).
22. Apostolova I, Steffen IG, Wedel F, Lougovski A, Marnitz S, Derlin T, et al. Asphericity of pretherapeutic tumour FDG uptake provides independent prognostic value in head-and-neck cancer. *European radiology*. 2014; 24(9):2077–87. <https://doi.org/10.1007/s00330-014-3269-8> PMID: 24965509

23. Eisenhauer E, Therasse P, Bogaerts J, Schwartz L, Sargent D, Ford R, et al. New response evaluation criteria in solid tumours: revised RECIST guideline (version 1.1). *European journal of cancer*. 2009; 45(2):228–47. <https://doi.org/10.1016/j.ejca.2008.10.026> PMID: 19097774
24. Yin J, Tian L. Joint confidence region estimation for area under ROC curve and Youden index. *Statistics in Medicine*. 2014; 33(6):985–1000. <https://doi.org/10.1002/sim.5992> PMID: 24123069
25. Ganeshan B, Panayiotou E, Burnand K, Dizdarevic S, Miles K. Tumour heterogeneity in non-small cell lung carcinoma assessed by CT texture analysis: a potential marker of survival. *European radiology*. 2012; 22(4):796–802. <https://doi.org/10.1007/s00330-011-2319-8> PMID: 22086561
26. Mayerhoefer ME, Schima W, Trattning S, Pinker K, Berger-Kulemann V, Ba-Ssalamah A. Texture-based classification of focal liver lesions on MRI at 3.0 Tesla: A feasibility study in cysts and hemangiomas. *Journal of Magnetic Resonance Imaging*. 2010; 32(2):352–9. <https://doi.org/10.1002/jmri.22268> PMID: 20677262
27. O'connor J, Rose C, Jackson A, Watson Y, Cheung S, Maders F, et al. DCE-MRI biomarkers of tumour heterogeneity predict CRC liver metastasis shrinkage following bevacizumab and FOLFOX-6. *British journal of cancer*. 2011; 105(1):139. <https://doi.org/10.1038/bjc.2011.191> PMID: 21673686
28. Hatt M, Majdoub M, Vallières M, Tixier F, Le Rest CC, Groheux D, et al. 18F-FDG PET uptake characterization through texture analysis: investigating the complementary nature of heterogeneity and functional tumor volume in a multi-cancer site patient cohort. *Journal of Nuclear Medicine*. 2015; 56(1):38–44. <https://doi.org/10.2967/jnumed.114.144055> PMID: 25500829
29. Lapa C, Werner RA, Schmid J-S, Papp L, Zsótér N, Biko J, et al. Prognostic value of positron emission tomography-assessed tumor heterogeneity in patients with thyroid cancer undergoing treatment with radiopeptide therapy. *Nuclear medicine and biology*. 2015; 42(4):349–54. <https://doi.org/10.1016/j.nucmedbio.2014.12.006> PMID: 25595135
30. Pelosi G, Bresaola E, Bogina G, Pasini F, Rodella S, Castelli P, et al. Endocrine tumors of the pancreas: Ki-67 immunoreactivity on paraffin sections is an independent predictor for malignancy: a comparative study with proliferating-cell nuclear antigen and progesterone receptor protein immunostaining, mitotic index, and other clinicopathologic variables. *Hum Pathol*. 1996; 27(11):1124–34. PMID: 8912819.
31. Ferrone CR, Tang LH, Tomlinson J, Gonen M, Hochwald SN, Brennan MF, et al. Determining Prognosis in Patients With Pancreatic Endocrine Neoplasms: Can the WHO Classification System Be Simplified? *Journal of Clinical Oncology*. 2007; 25(35):5609–15. <https://doi.org/10.1200/JCO.2007.12.9809> PMID: 18065733.
32. Khan MS, Luong TV, Watkins J, Toumpanakis C, Caplin ME, Meyer T. A comparison of Ki-67 and mitotic count as prognostic markers for metastatic pancreatic and midgut neuroendocrine neoplasms. *British Journal of Cancer*. 2013; 108(9):1838–45. <https://doi.org/10.1038/bjc.2013.156> PMC3658531. PMID: 23579216
33. Chan DL, Clarke SJ, Diakos CI, Roach PJ, Bailey DL, Singh S, et al. Prognostic and predictive biomarkers in neuroendocrine tumours. *Critical Reviews in Oncology/Hematology*. 2017; 113:268–82. <https://doi.org/10.1016/j.critrevonc.2017.03.017> PMID: 28427516
34. Rindi G, Klöppel G, Couvelard A, Komminoth P, Körner M, Lopes J, et al. TNM staging of midgut and hindgut (neuro) endocrine tumors: a consensus proposal including a grading system. *Virchows Archiv*. 2007; 451(4):757–62. <https://doi.org/10.1007/s00428-007-0452-1> PMID: 17674042
35. Yang Z, Tang LH, Klimstra DS. Effect of tumor heterogeneity on the assessment of Ki67 labeling index in well-differentiated neuroendocrine tumors metastatic to the liver: implications for prognostic stratification. *The American journal of surgical pathology*. 2011; 35(6):853–60. <https://doi.org/10.1097/PAS.0b013e31821a0696> PMID: 21566513
36. Singh S, Hallet J, Rowsell C, Law C. Variability of Ki67 labeling index in multiple neuroendocrine tumors specimens over the course of the disease. *European Journal of Surgical Oncology (EJSO)*. 2014; 40(11):1517–22.
37. Yao JC, Phan AT, Chang DZ, Wolff RA, Hess K, Gupta S, et al. Efficacy of RAD001 (everolimus) and octreotide LAR in advanced low-to intermediate-grade neuroendocrine tumors: results of a phase II study. *Journal of Clinical Oncology*. 2008; 26(26):4311–8. <https://doi.org/10.1200/JCO.2008.16.7858> PMID: 18779618
38. Brabander T, van der Zwan WA, Teunissen JJ, Kam BL, de Herder WW, Feelders RA, et al. Pitfalls in the response evaluation after peptide receptor radionuclide therapy with [177Lu-DOTA0, Tyr3] octreotate. *Endocrine-Related Cancer*. 2017; 24(5):243–51. <https://doi.org/10.1530/ERC-16-0524> PMID: 28320783
39. Brabander T, van der Zwan WA, Teunissen JJM, Kam BLR, Feelders RA, de Herder WW, et al. Long-Term Efficacy, Survival, and Safety of [(177)Lu-DOTA(0), Tyr(3)]octreotate in Patients with Gastroenteropancreatic and Bronchial Neuroendocrine Tumors. *Clinical cancer research: an official journal of the*

- American Association for Cancer Research. 2017; 23(16):4617–24. Epub 2017/04/22. <https://doi.org/10.1158/1078-0432.CCR-16-2743> PMID: 28428192.
40. Sabet A, Haslerud T, Pape U-F, Sabet A, Ahmadzadehfar H, Grünwald F, et al. Outcome and toxicity of salvage therapy with <sup>177</sup>Lu-octreotate in patients with metastatic gastroenteropancreatic neuroendocrine tumours. *European journal of nuclear medicine and molecular imaging*. 2014; 41(2):205–10. <https://doi.org/10.1007/s00259-013-2547-z> PMID: 24030668
  41. Knigge U, Capdevila J, Bartsch D, Baudin E, Falkerby J, Kianmanesh R, et al. ENETS Consensus Recommendations for the Standards of Care in Neuroendocrine Neoplasms: Follow-Up and Documentation. *Neuroendocrinology*. 2017; 105(2).
  42. Falconi M, Eriksson B, Kaltsas G, Bartsch D, Capdevila J, Caplin M, et al. ENETS consensus guidelines update for the management of patients with functional pancreatic neuroendocrine tumors and non-functional pancreatic neuroendocrine tumors. *Neuroendocrinology*. 2016; 103(2):153–71. <https://doi.org/10.1159/000443171> PMID: 26742109
  43. Ljungberg M, Pretorius PH. SPECT/CT: an update on technological developments and clinical applications. *The British journal of radiology*. 2017; 90(0):20160402.